Correction

MEDICAL SCIENCES

Correction for "Hepatic gap junctions amplify alcohol liver injury by propagating cGAS-mediated IRF3 activation," by Jay Luther, Sanjoy Khan, Manish K. Gala, Dmitry Kedrin, Gautham Sridharan, Russell P. Goodman, John J. Garber, Ricard Masia, Erik Diagacomo, Daniel Adams, Kevin R. King, Samuel Piaker, Hans-Christian Reinecker, Martin L. Yarmush, Josepmaria Argemi, Ramon Bataller, Jules L. Dienstag, Raymond T. Chung, and Suraj J. Patel, which was first published May 11, 2020; 10.1073/pnas.1911870117 (*Proc. Natl. Acad. Sci. U.S.A.* **117**, 11667–11673).

The authors note that the author name Dmitry Kedrin should instead appear as Dmitriy Kedrin. The corrected author line appears below. The online version has been corrected.

Jay Luther, Sanjoy Khan, Manish K. Gala, Dmitriy Kedrin, Gautham Sridharan, Russell P. Goodman, John J. Garber, Ricard Masia, Erik Diagacomo, Daniel Adams, Kevin R. King, Samuel Piaker, Hans-Christian Reinecker, Martin L. Yarmush, Josepmaria Argemi, Ramon Bataller, Jules L. Dienstag, Raymond T. Chung, and Suraj J. Patel

First published July 6, 2020.

www.pnas.org/cgi/doi/10.1073/pnas.2010186117

Hepatic gap junctions amplify alcohol liver injury by propagating cGAS-mediated IRF3 activation

Jay Luther[a,b,c], Sanjoy Khan[a], Manish K. Gala[a,b], Dmitriy Kedrin[a], Gautham Sridharan[d,e], Russell P. Goodman[a], John J. Garber[a], Ricard Masia[f], Erik Diagacomo[a], Daniel Adams[g], Kevin R. King[h], Samuel Piaker[a], Hans-Christian Reinecker[a], Martin L. Yarmush[d,e], Josepmaria Argemi[i,j], Ramon Bataller[i,j], Jules L. Dienstag[a], Raymond T. Chung[a], and Suraj J. Patel[a,c,k,1]

[a]Division of Gastroenterology, Department of Medicine, Massachusetts General Hospital, Harvard Medical School, Boston, MA 02114; [b]Clinical and Translational Unit, Department of Medicine, Massachusetts General Hospital, Harvard Medical School, Boston, MA 02114; [c]Alcohol Liver Center, Massachusetts General Hospital, Harvard Medical School, Boston, MA 02114; [d]Center for Engineering in Medicine, Department of Surgery, Massachusetts General Hospital, Boston, MA 02114; [e]Shriners Burns Hospital, Boston, MA 02114; [f]Pathology Unit, Massachusetts General Hospital, Harvard Medical School, Boston, MA 02114; [g]Heprotech Inc., Cambridge, MA 02139; [h]Division of Cardiovascular Medicine, University of California San Diego, La Jolla, CA 92093; [i]Division of Gastroenterology, Hepatology and Nutrition, Center for Liver Diseases, University of Pittsburgh, Pittsburgh, PA 15260; [j]Pittsburgh Liver Research Center, University of Pittsburgh, Pittsburgh, PA 15260; and [k]Division of Endocrinology, Department of Medicine, Beth Israel Deaconess Medical Center, Harvard Medical School, Boston, MA 02215

Edited by Charles M. Rice, Rockefeller University, New York, NY, and approved March 4, 2020 (received for review July 14, 2019)

Alcohol-related liver disease (ALD) accounts for the majority of cirrhosis and liver-related deaths worldwide. Activation of IFN-regulatory factor (IRF3) initiates alcohol-induced hepatocyte apoptosis, which fuels a robust secondary inflammatory response that drives ALD. The dominant molecular mechanism by which alcohol activates IRF3 and the pathways that amplify inflammatory signals in ALD remains unknown. Here we show that cytoplasmic sensor cyclic guanosine monophosphate-adenosine monophosphate (AMP) synthase (cGAS) drives IRF3 activation in both alcohol-injured hepatocytes and the neighboring parenchyma via a gap junction intercellular communication pathway. Hepatic RNA-seq analysis of patients with a wide spectrum of ALD revealed that expression of the cGAS-IRF3 pathway correlated positively with disease severity. Alcohol-fed mice demonstrated increased hepatic expression of the cGAS-IRF3 pathway. Mice genetically deficient in cGAS and IRF3 were protected against ALD. Ablation of cGAS in hepatocytes only phenocopied this hepatoprotection, highlighting the critical role of hepatocytes in fueling the cGAS-IRF3 response to alcohol. We identified connexin 32 (Cx32), the predominant hepatic gap junction, as a critical regulator of spreading cGAS-driven IRF3 activation through the liver parenchyma. Disruption of Cx32 in ALD impaired IRF3-stimulated gene expression, resulting in decreased hepatic injury despite an increase in hepatic steatosis. Taken together, these results identify cGAS and Cx32 as key factors in ALD pathogenesis and as potential therapeutic targets for hepatoprotection.

IRF3 | cGAS | innate immunity | connexin | alcohol liver

Alcohol-related liver disease (ALD) affects over 150 million people worldwide and exacts a substantial toll of morbidity and mortality. In the United States, ALD accounts for approximately half of cirrhosis-related deaths and is currently the second leading reason for liver transplantation (1). Moreover, the most severe form of ALD, acute alcoholic hepatitis (AH), carries a 6-mo mortality rate as high as 40% (2). While the primary goal of ALD management is abstinence, such self-restraint is notoriously difficult to achieve and sustain, and recidivism rates are high. Furthermore, no FDA approved therapies are currently available for ALD. As a result, there is an urgent and unmet need to identify novel biological drivers of the disease and develop effective therapeutics.

Although the pathogenesis of ALD is complex, dysregulated activation of innate immunity and an overexuberant sterile inflammatory response have been demonstrated to contribute to liver injury in ALD (3–5). Oxidative stress, mitochondrial injury, and enhanced intestinal permeability have been well documented in establishing the host inflammatory response elicited in ALD (6, 7); however, the exact mechanism by which ethanol damages hepatocytes at the most proximal level, which then triggers this cascade of events, remains unknown. A recent advance in our understanding of innate immunity was the identification of cyclic guanosine monophosphate-adenosine monophosphate (AMP) synthase (cGAS) as a critical regulator of host response to cellular injury (8). cGAS is a DNA sensor that triggers innate immune responses through production of the secondary messenger cyclic 2′3′-cGAMP, which binds and activates stimulator of interferon (IFN) genes (STING), resulting in IFN regulatory factor 3 (IRF3) activation (8). Originally identified as a key defense mediator against infectious diseases, cGAS has now been implicated in several disease states, including inflammatory, metabolic, and neoplastic processes (9–12). While the role of cGAS in ALD is unknown, the essential contribution of IRF3 in ALD has been previously demonstrated. IRF3-deficient mice exposed to alcohol exhibit attenuated hepatocyte apoptosis, inflammation, and

Significance

Alcohol-related liver disease is a leading cause of mortality worldwide. Improved patient outcomes will be driven by advances in our understanding of disease pathogenesis, allowing for the development of novel, targeted therapeutics. By combining patient data with animal models of alcohol-related liver disease, we demonstrate the critical importance of the cyclic guanosine monophosphate–adenosine monophosphate synthase-interferon regulatory factor 3 (cGAS-IRF3) pathway and its amplification through hepatocyte intercellular communication in fueling liver injury caused by alcohol. Thus, our results identify two potentially druggable pathways to improve patient outcomes and reduce mortality resulting from this devastating disease.

Author contributions: J.L., E.D., D.A., and S.J.P. designed research; J.L., S.K., G.S., J.J.G., R.M., E.D., D.A., S.P., J.A., R.B., and S.J.P. performed research; J.L., J.J.G., R.M., K.R.K., H.-C.R., and S.J.P. contributed new reagents/analytic tools; J.L., M.K.G., D.K., R.P.G., R.M., K.R.K., M.L.Y., J.L.D., and S.J.P. analyzed data; and J.L., M.K.G., D.K., R.P.G., M.L.Y., R.T.C., and S.J.P. wrote the paper.

Competing interest statement: The authors declare a competing interest. K.R.K., M.Y.L., and S.J.P. have equity interest in Heprotech Inc. M.K.G. has equity interest in New Amsterdam Genomics. All other authors have no conflicts to declare.

This article is a PNAS Direct Submission.

[1]To whom correspondence may be addressed. Email: sjpatel32@mgh.harvard.edu.

This article contains supporting information online at https://www.pnas.org/lookup/suppl/doi:10.1073/pnas.1911870117/-/DCSupplemental.

First published May 11, 2020.

liver injury independent of IRF3's classical role as a transcription factor for IFN-stimulated genes (ISGs) (13). However, certain fundamental questions remain regarding 1) the contribution of cGAS to IRF3 activation and liver injury in ALD, 2) the mechanism by which IRF3 activation is amplified in ALD, and 3) the role of activation of the cGAS-IRF3 pathway in patients with ALD.

One way cells spread IRF3 signals is through gap junctions. Gap junctions are intercellular channels composed of connexin proteins that directly connect the cytosol of adjacent cells, thereby allowing rapid propagation of cellular signals (14). We have previously shown that gap junction communication between cells plays a pivotal role in amplifying innate immunity and host defense (15). Mechanistically, gap junctions facilitate intercellular transfer of 2′3′-cGAMP from injured to bystander cells, amplifying IRF3 activation across cells (16). Although these investigations were limited to in vitro models, recent in vivo studies have highlighted the importance of gap junctions in establishing liver injury. For example, deficiency in connexin 32 (Cx32), the predominant hepatic gap junction, attenuates injury in several murine models of liver disease (17–19). Despite these compelling data, the role of Cx32 in ALD and its ability to modulate IRF3 in vivo have not been studied.

Here, we show that alcohol activates the cGAS-IRF3 pathway in murine models of ALD and positively correlates with disease severity in patients with ALD. We also demonstrate that mice deficient in hepatocyte cGAS are protected against ALD, suggesting that the liver parenchyma plays a critical role in establishing alcohol-induced liver injury. Furthermore, blocking of Cx32 prevents the amplification of IRF3 activation and downstream oxidative stress, inflammation, and liver injury in murine models of ALD. Taken together, our results identify a pathway critical to ALD pathogenesis in both mice and humans.

Results

Alcohol Activates the cGAS-IRF3 Pathway. To determine if the cGAS-IRF3 pathway is altered in human ALD, we studied hepatic expression of this pathway in patients with ALD. We analyzed RNA-seq data from human liver samples that were obtained from the InTeam Consortium's Human Biorepository Core (20). This cohort consists of 51 patients with a wide spectrum of ALD (Table 1), including those with no liver injury and those with varying degrees of steatohepatitis. Gene set enrichment analysis of this transcriptomic data revealed that, in patients with ALD, biological pathways related to IRF3 were significantly altered (Fig. 1*A*). Furthermore, when we examined patients based on disease severity (Fig. 1*B*), we found that IRF3 and IRF3-related gene expression correlated quantitatively with disease severity. Specifically, expression of cGAS, TANK-binding kinase 1 (TBK1), IkappaB kinase-epsilon (IKKε), STING, and IRF3 correlated positively with the severity of ALD (Fig. 1*C*). Consistent with activation of this pathway, IFN-stimulated genes were also up-regulated significantly in patients with ALD compared to healthy controls (Fig. 1*C*). Additionally, negative regulators of the cGAS-IRF3 pathway, such as ectonucleotide pyrophosphatase/phosphodiesterase 1 (ENPP1), were down-regulated in patients with ALD (Fig. 1*C*). A similar pattern of gene expression was noted in primary human hepatocytes exposed in vitro to alcohol (*SI Appendix*, Fig. S1). These data in humans show a correlation between activation of the cGAS-IRF3 pathway and severity of ALD.

To investigate the role of the cGAS-IRF3 pathway in mice, we fed mice the Lieber-DeCarli diet, a classic model for studying alcohol-induced liver injury (21). We found that protein levels of cGAS, TBK1, IRF3, and phosphorylated IRF3 (pIRF3) were elevated markedly in liver tissue of alcohol-fed mice (Fig. 1*D*). Consistent with these findings, we found that hepatic mRNA

Table 1. Baseline characteristics of patients and controls at time of liver biopsy

	Normal livers, $n = 10$	Early ASH, $n = 12$	Nonsevere AH, $n = 11$	Severe AH, $n = 18$	Kruskal-Wallis test/ χ^2 test
Demographics					
Age–median (IQR)	32 (29.0–49.0)	52 (48.8–58.2)	46 (42.5–49.5)	51 (47.2–57.8)	0.363
Gender–male *n* (%)	7 (70)	7 (58.3)	7 (63.6)	11 (61.1)	0.949
Severity scores–median (IQR)					
Child-Pugh	N/A	N/A	7 (6–8.5)	11 (9–11.8)	0.000
MELD	N/A	N/A	12 (10.5–14.5)	24 (22–27.8)	0.001
ABIC	N/A	N/A	6 (5.5–6.4)	8.3 (7.9–8.8)	0.000
Decompensations–*n* (%)					
Ascites	0	0	5 (45.5)	13 (72.2)	0.240
Hepatic encephalopathy	0	0	0 (0)	5 (27.8)	0.126
Upper GI bleeding	0	0	1 (9.1)	1 (5.6)	1
Acute kidney injury	0	0	2 (18.2)	9 (50)	0.125
Infections	0	0	1 (9.1)	6 (33.3)	0.202
Lab parameters–median (IQR)					
Hemoglobin (g/dL)	14.6 (13.2–15.3)	14.3 (13.7–16.1)	11.8 (9.8–13.3)	11.5 (11.0–12.7)	0.000
WBC x 109/L	5.7 (5.2–7.1)	5.6 (4.7–6.9)	6.7 (5.3–7.7)	9.6 (8.1–14.3)	0.000
Platelets x 109/L	237 (217–267.5)	189.5 (131.8–236.2)	166 (104–208.5)	115 (82.2–183.5)	0.011
AST (U/L)	21.5 (19.2–25.8)	107 (66–142)	104 (51–196.5)	133 (117.5–218.2)	0.000
ALT (U/L)	25 (16.8–31.2)	70.0 (58.5–89.2)	36 (30.5–45)	55 (35–65.5)	0.001
Bilirubin (mg/dL)	0.6 (0.5–0.7)	1.2 (0.8–1.4)	1.7 (0.9–3.2)	19 (12.9–26.2)	0.000
GGT (U/L)	17 (14.0–23.2)	388 (208.2–674.5)	709 (274.5–1202.5)	293.5 (175.5–456.8)	0.000
ALP (U/L)	147 (112.5–184.8)	89.5 (70.0–117.2)	393 (249.5–531)	402 (300.5–494.8)	0.005
Albumin (g/dL)	4.6 (4.4–4.6)	4.5 (4.2–4.7)	3.2 (2.9–3.7)	2.5 (2.3–3.0)	0.000
Creatinine (mg/dL)	0.84 (0.76–0.89)	0.6 (0.59–0.73)	0.69 (0.60–0.86)	1.02 (0.73–1.31)	0.102
Sodium (mEq/L)	140.0 (139.2–141.0)	139.5 (137.5–140.0)	137 (135–138)	132.0 (130.2–136.5)	0.001
INR	1.02 (0.99–1.05)	0.99 (0.94–1.02)	1.25 (1.15–1.43)	1.67 (1.56–1.81)	0.000

WBC: white blood count; GGT: gamma-glutamyl transpeptidase; ALP: alkaline phosphatase; INR: international normalized ratio; IQR: interquartile range; ABIC: age–bilirubin–INR–creatinine score; N/A: not applicable.

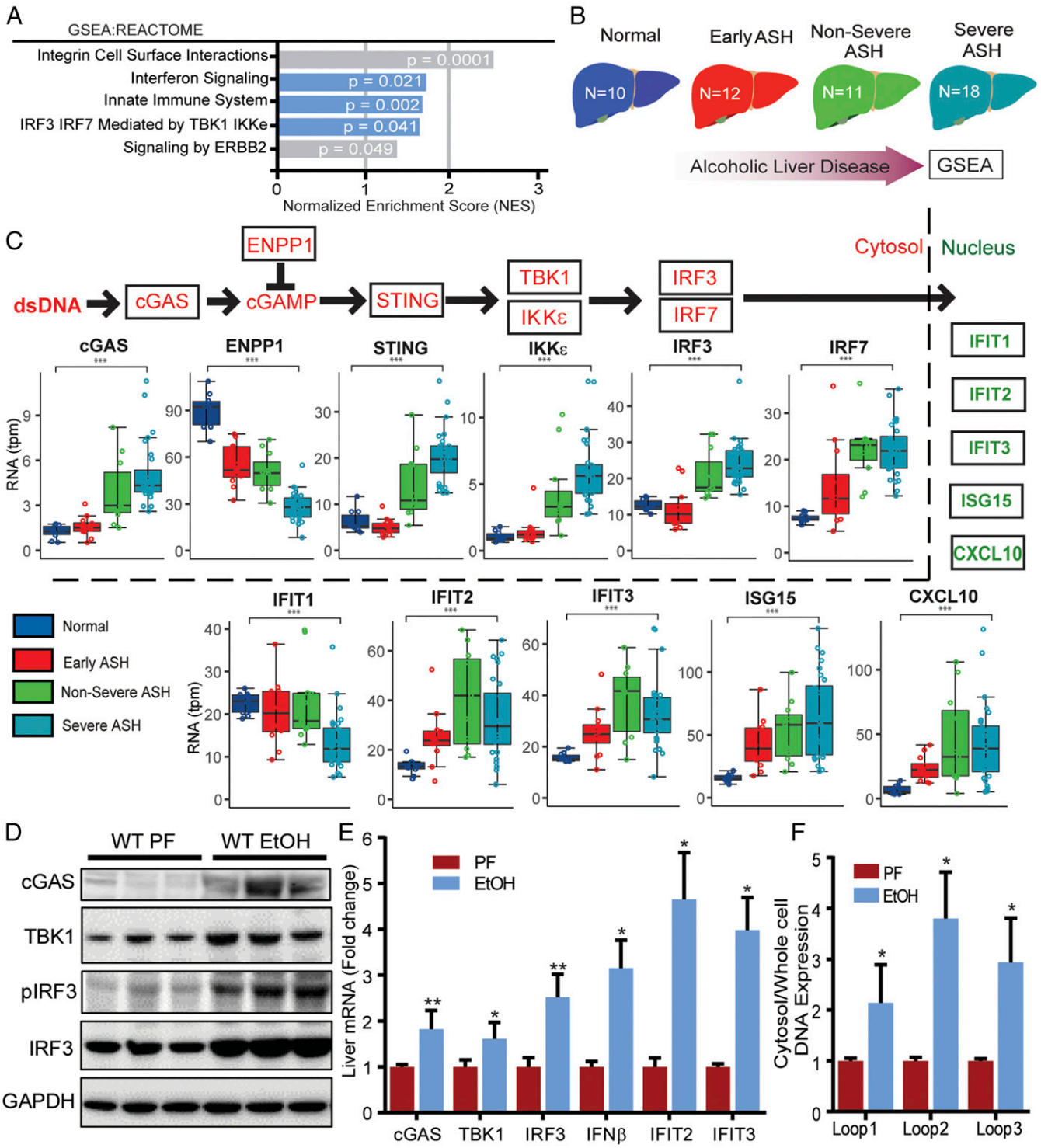

Fig. 1. Alcohol activates the cGAS-IRF3 pathway in humans and mice. (*A*) GSEA of RNA-seq expression data from liver tissue of healthy controls and patients with alcohol-related liver disease (ALD). The enrichment score (ES) reflects the degree to which a gene set is overrepresented at the top or bottom of a ranked list of genes. (*B*) Schematic depicting the spectrum of disease severity within the ALD patient cohort. (*C*, *Top*) Abbreviated schematic of the cGAS-IRF3 pathway (red) and downstream IRF3-regulated genes (green). (*C*, *Bottom*) Differential expression analysis of cGAS-IRF3 pathway and IRF3-regulated genes based on disease severity within the ALD patient cohort. WT mice were fed 5% alcohol (EtOH) or a control PF diet for 6 wk. (*D*) Immunoblot for cGAS, TBK1, pIRF3, IRF3, and GAPDH and (*E*) hepatic mRNA expression of *cGas*, *Tbk1*, *Irf3*, and IRF3-regulated genes (*Ifnβ*, *Ifit2*, *Ifit3*) from EtOH and PF WT liver tissue. DNA in the cytosolic fraction hepatocytes from WT ETOH- and PF-fed mice was isolated, and the relative abundance of mtDNA was measured by RT-PCR normalized to whole-cell extract. (*F*) Cytosolic mtDNA content in liver tissue from WT and PF mice. $N = 10$ mice/group. Data are shown as mean ± SD. $^{*}P < 0.05$; $^{**}P < 0.01$; $^{***}P < 0.001$.

expression of *cGas*, *Tbk1*, *Irf3*, and multiple ISGs was upregulated in alcohol-fed mice (Fig. 1*E*). Next, we investigated for potential activators of cGAS. While cGAS is known to be activated by mitochondrial DNA (mtDNA) (22), whether alcohol can induce mitochondrial injury sufficient to trigger leakage of mtDNA into the cytoplasm is unknown. To address this

question, we purified total DNA from the cytosolic fraction of hepatocytes isolated from alcohol-fed and pair-fed (PF) mice. We found that alcohol-fed mice had significantly increased cytoplasmic mtDNA levels compared to PF controls (Fig. 1*F*). Taken together, our murine and human data show that alcohol activates the cGAS-IRF3 pathway in the liver.

cGAS Deficiency Protects against Alcohol-Induced IRF3 Activation and Liver Injury. To determine the necessity of cGAS in establishing alcohol-induced IRF3 activation and liver injury, we exposed cGAS-deficient (cGAS knockout [KO]) mice to alcohol. Despite consuming similar amounts of alcohol and exhibiting comparable serum ethanol levels (*SI Appendix*, Fig. S2), cGAS KO mice demonstrated a marked reduction in IRF3 activation, as reflected by lower expression of ISGs, compared to alcohol-fed wild-type (WT) mice (Fig. 2*A*). Notably, this reduction was similar to that seen in IRF3-deficient (IRF3 KO) mice, suggesting that alcohol-induced IRF3 activation requires cGAS. Consistent with this conclusion, we found that alcohol-fed cGAS KO mice had significantly lower levels of serum aminotransferase (alanine aminotransferase [ALT] and alanine aminotransferase [AST]) and substantially less histological evidence of liver injury compared to WT mice, based on the degree of steatosis and inflammation present (Fig. 2 *B*–*E*). Deficiency in STING, an intermediate in the cGAS-IRF3 pathway, also protected against liver injury (*SI Appendix*, Fig. S3). Collectively, these findings show that alcohol-induced IRF3 activation and liver injury require cGAS.

Next, we sought to determine the specific cell type responsible for hepatic cGAS-IRF3 induction by alcohol. To accomplish this, we generated hepatocyte-specific cGAS-deficient mice with the Cre-Lox system. Mice expressing a floxed *cGas* exon 2 (cGAS F/F) were backcrossed to C57BL/6J mice and then crossed with albumin-Cre mice to create mice with cGAS deficiency only in hepatocytes (cGAS LKO). The outcome of this cross was confirmed by mRNA assessment and immunoblot (Fig. 2*F*). We found that alcohol-fed cGAS LKO mice exhibited a similar reduction in ALT, AST, and histological evidence of inflammation and injury compared to cGAS KO mice (Fig. 2 *G*–*I* and *SI Appendix*, Fig. S2), suggesting that hepatocytes are the primary cell type responsible for alcohol-induced cGAS-IRF3 activation.

Cx32 Deficiency Limits 2′3′-cGAMP Propagation and Alcohol-Induced IRF3 Activation in Liver. Thus far, our data highlight the importance of hepatocyte-specific cGAS-IRF3 activation in triggering liver injury caused by alcohol. Hepatocytes are intricately connected by Cx32 gap junctions that are capable of propagating multiple danger signals, including those responsible for amplifying IRF3 activation (15, 16). We asked if hepatocytes can spread 2′3′-cGAMP from stimulated cells to activate IRF3 in bystander cells and if this propagation is dependent on Cx32. Hepatocyte-derived H35 cells were stimulated with a vehicle control or 2′3′-cGAMP (donor cells), trypsinized, thoroughly washed, and transplanted onto unstimulated H35 IRF3-green fluorescent protein (GFP) reporter cells that express GFP upon IRF3 activation. We found that IRF3-GFP reporters were activated after coculture with 2′3′-cGAMP–treated donor cells. In contrast, no IRF3 activity was observed in the reporters in the presence of 2APB, a known small molecule inhibitor of Cx32 (Fig. 3 *A* and *B*).

To understand if disruption of Cx32 affects alcohol-induced activation of IRF3, we exposed Cx32-deficient mice (Cx32KO) to the chronic and binge ethanol dietary model. Despite similar consumption of alcohol and serum ethanol levels (*SI Appendix*, Fig. S2), Cx32KO mice demonstrated a significant reduction in hepatic phosphorylated TBK1 (pTBK1) and pIRF3 compared to their littermate WT controls (Fig. 3*C*). The hepatic expression of several ISGs was also markedly reduced in Cx32KO mice (Fig. 3*D*). Alcohol-induced IRF3 activation has been shown to induce hepatocyte apoptosis (13); consistent with this expectation, Cx32KO mice demonstrated lower levels of hepatocyte apoptosis (Fig. 3 *E* and *F*). Pathway enrichment analysis (PEA) of hepatic transcriptomic data comparing alcohol-fed WT versus PF WT mice revealed apoptosis as one of the most significantly perturbed pathways ($P < 10^{-5}$). However, this pathway was not perturbed when comparing alcohol-fed Cx32KO versus PF Cx32KO mice, suggesting that fewer apoptosis genes were expressed differentially with alcohol treatment. Specifically, 42 of 84 genes cataloged under "Apoptosis Signaling" were expressed differentially with alcohol treatment ($P = 6 \times 10^{-6}$) in WT mice, while only 27 genes were expressed differentially in the Cx32KO mice ($P = 0.079$). Interestingly, PEA revealed that, out of the 25 most differentially regulated pathways (based on *P* value) in WT mice receiving alcohol, 6 were not perturbed in Cx32 KO mice (Fig. 3*G*), including apoptosis. Collectively, these data demonstrate the importance of Cx32 in amplifying alcohol-induced IRF3 activation and apoptosis in the liver.

Cx32 Deficiency Limits Alcohol-Induced Hepatocyte Injury and Inflammation. Knowing that Cx32 deficiency limits alcohol-induced IRF3 activation, we sought to determine if this observation

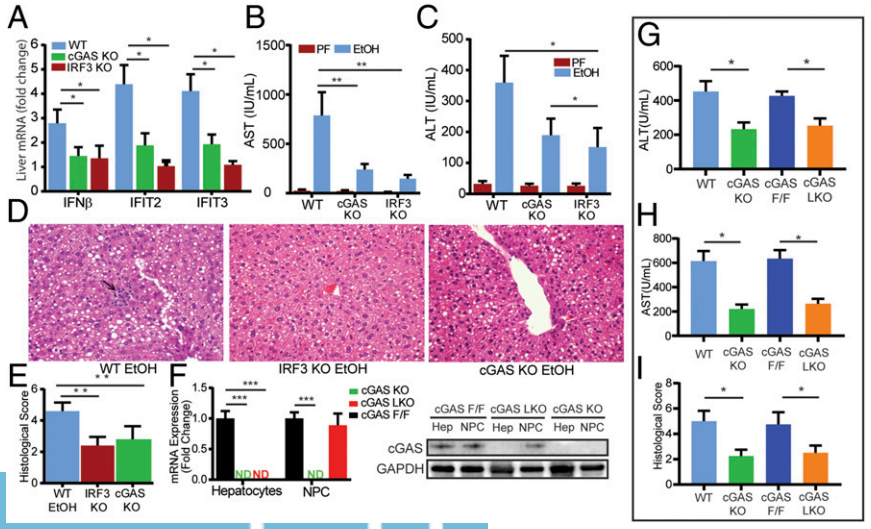

Fig. 2. Hepatocyte-specific cGAS drives alcohol-induced IRF3 activation and liver injury. WT, cGAS-deficient (cGAS KO), and IRF3-deficient (IRF3 KO) mice were exposed to the 10-d NIAAA chronic and binge alcohol model. (*A*) Hepatic mRNA expression of IRF3-regulated genes (*Ifnβ*, *Ifit2*, *Ifit3*), (*B* and *C*) serum transaminase levels, and (*D* and *E*) liver histology and histological scoring (hematoxylin and eosin [H&E], 40× magnification; arrow highlighting an inflammatory foci) from WT, cGAS KO, and IRF3 KO mice. (*F*) mRNA expression and immunoblot for *cGas* in hepatocytes and nonparenchymal cells (NPCs) from cGAS F/F, cGAS KO, and cGAS LKO mice. (*G* and *H*) Serum transaminase levels and (*I*) histological score from WT, cGAS KO, cGAS F/F, and cGAS LKO mice exposed to the NIAAA chronic and binge alcohol model. N = 6–10 mice/group. Data are shown as mean ± SD. *$P < 0.05$; **$P < 0.01$; ***$P < 0.001$.

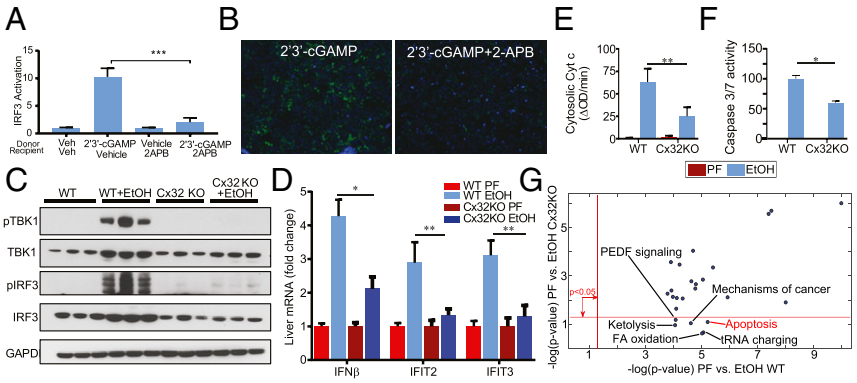

Fig. 3. Cx32 amplifies alcohol-induced IRF3 activation and apoptosis. Hepatocyte-derived H35 cells were stimulated with 2′3′-cGAMP or vehicle (donor cells) and cocultured with unstimulated or 2APB–treated H35 IRF3-GFP reporter cells (recipient cells) that express GFP upon IRF3 activation. (*A*) IRF3 activity as determined by flow cytometry and (*B*) representative 20× fluorescence images of 2′3′-cGAMP–stimulated H35 cells cocultured with H35 GFP reporter cells in the presence or absence of 2APB (green = GFP, blue = DAPI). Cx32KOmice and their littermate controls (WT) were exposed to the 10-d NIAAA chronic and binge alcohol model. (*C*) Immunoblot for phosphorylated TBK1 (pTBK1), TBK1, pIRF3, IRF3, and GAPDH, (*D*) hepatic mRNA expression of IRF3-regulated genes (*Ifnβ*, *Ifit2*, *Ifit3*), (*E*) cytosolic cytochrome C activity, and (*F*) Caspase 3/7 in liver tissue from WT and Cx32KO mice. (*G*) Ingenuity pathway analysis (IPA) was used to analyze hepatic transcriptome data for the following two comparisons: 1) ethanol vs. sober for WT mice and 2) ethanol vs. sober for Cx32KO mice. PEA provided *P* values associated with a pathway based on Fisher's exact test and plotted in negative log scale for both comparisons. $N = 10$ mice/group. Data are shown as mean ± SD. $*P < 0.05$; $**P < 0.01$; $***P < 0.001$.

translated into hepatoprotection. We found that alcohol-fed Cx32KO mice exhibited significantly less liver injury compared to WT mice, demonstrated by fivefold and tenfold reductions in ALT and AST, respectively (Fig. 4 *A* and *B*). Furthermore, hepatic mRNA levels of key inflammatory cytokines and chemokines were lower in Cx32KO mice compared to WT mice (Fig. 4*C*). Consistent with less injury, hepatic metabolomic data demonstrated reduced exhaustion of important antioxidants (glutathione, s-adenylmethionine, and NADPH) in alcohol-fed Cx32KO compared to WT mice, suggesting less oxidative stress burden (Fig. 4*D* and *SI Appendix*, Fig. S4). We were able to replicate this observed hepatoprotection with small-molecule inhibition (2APB) of Cx32 in mice exposed to the chronic and binge alcohol model (Fig. 4*E*). In addition to a reduction in hepatocyte injury, inflammation, and oxidative stress, we observed a survival advantage in Cx32KO and 2APB-treated WT mice exposed to 6% ethanol (Fig. 4*F*). Collectively, these data show that Cx32 plays a critical role in determining the severity of alcohol-induced injury.

Cx32 Deficiency Induces Hepatic Triglyceride Accumulation and Up-Regulation of Glycerophosphodiester Phosphodiesterase Domain Containing 3. An unexpected yet remarkable finding from histological analysis of liver specimens from Cx32KO mice exposed to alcohol was a markedly increased burden of hepatic steatosis, confirmed both by oil red O staining and by hepatic triglyceride measurement (Fig. 5 *A* and *B*). The mechanism for this observation remained elusive, especially since Cx32 had not been previously linked to lipid metabolism. To address the mechanism, we evaluated the hepatic expression of key genes involved in de novo lipogenesis; triglyceride synthesis; and fatty acid oxidation, metabolism, uptake, and transport. Interestingly, we found no differences in these genes at the expression level in Cx32KO mice compared to their WT counterparts (*SI Appendix*, Fig. S5). Given these results, it appeared that the observed hepatic triglyceride accumulation in Cx32KO mice was not dependent on the classical regulators involved in lipid homeostasis.

Next, we analyzed hepatic mRNA microarray data from WT and Cx32KO mice to identify candidate drivers of triglcyeride accumulation observed in the alcohol-fed Cx32KO mice. Glycerophosphodiester phosphodiesterase domain containing 3 (GDPD3) was found to be the most up-regulated gene in Cx32KO mice (*SI Appendix*, Fig. S6). We validated this finding by real-time PCR and determined that the increased expression of GDPD3 in Cx32KO mice was localized to hepatocytes (*SI Appendix*, Fig. S7). Notably, inhibition of the Cx32 function by 2APB did not increase hepatic GDPD3 mRNA levels, in contrast to genetic deletion of Cx32 (*SI Appendix*, Fig. S8).

The identification of GDPD3 was of interest given its emerging role in choline metabolism, lipid handling, and triglyceride synthesis. To directly assess the effect of GDPD3 on hepatocyte fat accumulation, we used recombinant adenoviral vectors expressing GDPD3-GFP or GFP alone as a control. We confirmed up-regulation of hepatic GDPD3 in GDPD3-GFP–treated mice (*SI Appendix*, Fig. S9). We compared the amounts of steatosis and injury induced by the chronic and binge ethanol model in mice that received GDPD3-GFP or GFP control. We found that GDPD3-GFP–infected mice exposed to ethanol displayed no hepatic protection based on serum ALT levels (Fig. 5*C*). However, these mice did exhibit increased hepatic steatosis compared to control GFP-infected mice, based on histology and hepatic triglyceride measurement (Fig. 5 *D* and *E*). Notably, Cx32 expression was not altered in GDPD3-overexpressing mice (*SI Appendix*, Fig. S10). These data suggest that GDPD3 possibly contributes to the increased hepatic lipid accumulation observed in Cx32KO mice exposed to ethanol, but it likely plays no role in the hepatoprotective phenotype.

Discussion

In this report, we show that the cGAS-IRF3 pathway is activated in ALD in both mice and humans, and that this activation correlates with disease severity. Consistent with this conclusion, mice deficient in hepatocyte cGAS are protected against ALD. Furthermore, blocking intercellular transfer of cGAS-produced 2′3′-cGAMP through either pharmacologic or genetic inhibition of Cx32 prevents alcohol-induced IRF3 activation, oxidative stress, inflammation, and liver injury. Finally, we identified the potential role of GDPD3 in alcohol-induced hepatocyte lipid accumulation. Taken together, our results identify a pathway critical to ALD pathogenesis.

The important role of IRF3 in the pathogenesis of ALD has been studied previously. Activation of IRF3 is known to promote hepatocyte apoptosis through a pathway independent of its traditional role as a transcription factor for type I interferons. In ALD, IRF3 activation leads to an interaction of IRF3 with the proapoptotic BAX, causing hepatocyte apoptosis and setting the stage for inflammation and injury (13). Our data suggest that decreasing ALD-induced IRF3 activation results in less apoptosis and subsequently less liver injury. However, it is important to note that multiple other cell-death pathways exist, such as pyroptosis, nectroptosis, and necrosis, that may also contribute to ALD-induced liver injury. Further investigation is warranted to define the role of IRF3 in these other cell-death pathways.

Our data identify a potential upstream pathway that triggers IRF3 activation in ALD. We show the ability of alcohol to induce mitochondrial injury sufficient to cause leakage of

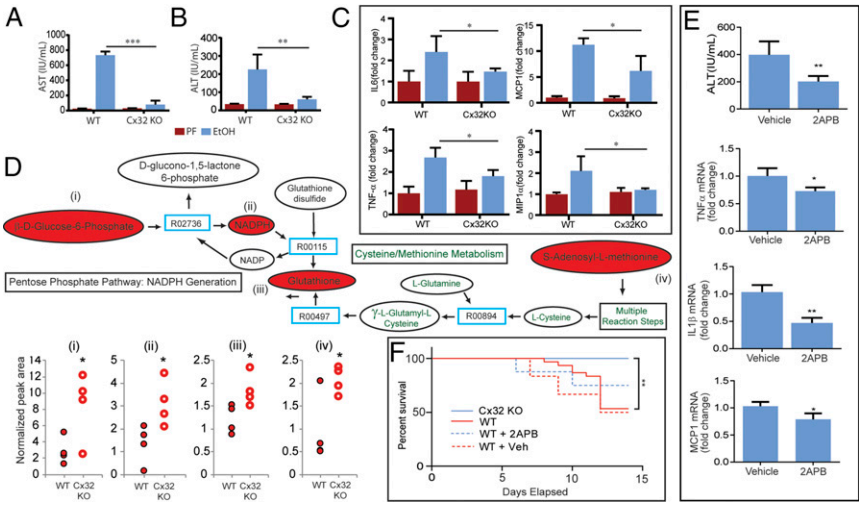

Fig. 4. Cx32 propagates alcohol-induced hepatocyte injury, inflammation, and mortality. WT and Cx32KO mice were exposed to the 10-d NIAAA chronic and binge ethanol model. (*A* and *B*) Serum transaminase levels and (*C*) hepatic mRNA expression of inflammatory genes (*Il6*, *Mcp1*, *Tnfα*, *Mip1α*) from WT and Cx32KO mice. (*D*) Hepatic metabolomic profiling of key mediators involved in oxidative stress pathways in WT and Cx32KO mice. (*E*) WT mice were exposed to the 10-d NIAAA chronic and binge ethanol model and treated with an intraperitoneal injection of 2APB (20 mg/kg) or vehicle control (dimethyl sulfoxide [DMSO], 0.1 mL/kg) prior to oral gavage of ethanol on day 10. Serum ALT and hepatic mRNA expression of inflammatory genes (*Il1β*, *Mcp1*, *Tfnα*). (*F*) Kaplan-Meier survival curve for 1) Cx32KO mice, 2) WT mice, 3) WT mice treated with daily 2APB injections (20 mg/kg), and 4) WT mice treated with daily vehicle injections of DMSO (0.1 mL/kg), exposed to a 6% ethanol diet. N = 6–10 mice/group. Data are shown as mean ± SD. $*P < 0.05$; $**P < 0.01$; $***P < 0.001$.

mtDNA into the cytoplasm. This critical step sets the stage for the activation of cGAS, induction of IRF3, and, ultimately, hepatocyte apoptosis. By identifying the most proximal steps in this pathway—namely, alcohol-induced mtDNA cytoplasmic leakage, and cGAS activation—our work establishes a pathway for ALD and, at the same time, reinforces the importance of mitochondrial injury and stress, which are classic drivers of ALD.

Furthermore, after establishing the importance of cGAS in ALD, we were able to identify the critical role of Cx32, a known modulator of the intercellular transfer of cGAS-produced 2′3′-cGAMP (15, 16). Previous work has established the important role of Cx32 in the inflammatory process of a variety of liver diseases, including drug-induced liver injury, nonalcoholic fatty liver disease, and ischemia-reperfusion injury (17–19). In the only published study of hepatic gap junctions in ALD, investigators examined the association of Cx32 in alcohol-related hepatocellular carcinoma and did not focus on inflammation (23). Despite these prior studies, the mechanism by which Cx32 contributes to these liver diseases has not been well established. We show that the ability of Cx32 to allow cell-to-cell transfer of 2′3′-cGAMP enhances the degree of IRF3 activation, hepatocyte apoptosis, and liver injury and inflammation in an in vivo model system. Whether this observation holds true for other forms of liver disease requires further study. In this case, by firewalling this amplification process, we were able to show that Cx32 deficiency could protect against ALD. This is of particular importance given the lack of effective therapeutics for ALD. Currently available treatments, including prednisolone, are only modestly effective, do not affect survival in the long term, and are not liver-specific, therefore coming with many substantial side-effects (24). In this work, we relied upon 2APB as a proof of concept that hepatic gap junctions may represent a druggable target, and we showed that transient inhibition of Cx32 protects against progression of inflammation by targeting a liver-specific protein without affecting immune cells. Prior to moving forward with a clinical program, further investigation is needed to develop a true Cx32 inhibitor with minimal off-target liabilities that have been attributed to 2APB.

Unexpectedly, Cx32KO mice demonstrated a marked increase in the burden of hepatic steatosis when exposed to alcohol, and our mechanistic studies suggested a role for *GDPD3* in driving this process. While the function of human *GDPD3* remains undefined, emerging data in mice highlight its role in lipid handling and triglyceride synthesis. Specifically, murine *GDPD3* exhibits lysophospholipase D activity against lysophosphatidyl choline (Lyso-PC) (25). Lyso-PC is critical for secretion of triglyceride from cells, likely through enhancement of apolipoprotein B (ApoB) and very low density lipoprotein (vLDL) production (26).

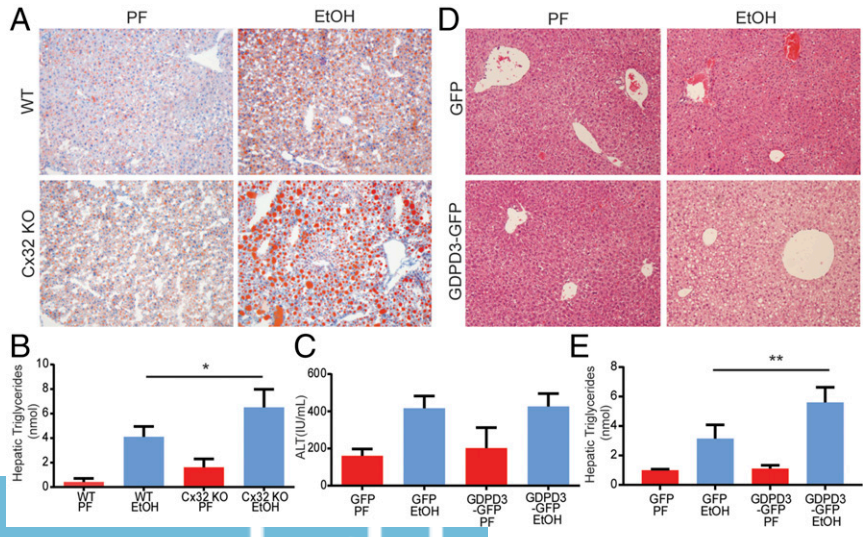

Fig. 5. Cx32 deficiency induces hepatic triglyceride accumulation and up-regulation of GDPD3. (*A* and *B*) WT and Cx32-deficient (Cx32KO) mice were exposed to the chronic and binge ethanol model. (*A*) Histological evidence of increased lipid deposition in Cx32KO mice compared to WT mice based on Oil Red O staining. (*B*) Increased hepatic triglyceride content in Cx32KO mice compared to WT mice. (*C*–*E*) WT mice were exposed to a modified version of the chronic and binge ethanol model, in which mice were injected on day 9 with either recombinant adenoviral vectors expressing GDPD3-GFP or GFP alone. Mice were then gavaged with 5 g ethanol/kg body weight on day 12 and killed 9 h later. (*C*) No difference in serum ALT in GDPD3-GFP–infected mice compared to control GFP-infected mice. (*D*) Increased steatosis based on histological analysis of H&E specimens. (*E*) Levels of hepatic triglycerides in GDPD3-GFP–infected mice compared to control GFP-infected mice. (Data are shown as mean ± SD and analyzed by Student's *t* tests. N = 8–12 mice/group. $*P < 0.05$; $**P < 0.01$; $***P < 0.001$.

Additionally, the product of murine *GDPD3* enzymatic activity is lysophosphatidic acid (LPA) (25). LPA plays many roles, including acting as a substrate for triglyceride syntheses (27). Therefore, *GDPD3* up-regulation is likely to affect triglyceride export by depleting Lyso-PC while also enhancing triglyceride synthesis through increased LPA production. It is important to note that transient inhibition of Cx32 by 2APB did not affect GDPD3 levels, suggesting that Cx32 regulation of GDPD3 is transcriptionally dependent. Further study of GDPD3's role in ALD is needed to determine its exact function in this disease process.

The study of ALD pathogenesis has been hampered by the lack of well-characterized cohorts of patients with ALD. This situation, in part, is related to a less compelling indication for liver biopsies in patients with alcohol hepatitis as compared to patients with other liver diseases, which limits the opportunity for hepatic expression data. A unique aspect of our study was that we were able to study hepatic expression levels of key steps in the cGAS-IRF3 pathway in patients with a wide spectrum of ALD. These analyses allowed us to identify variable expression of this pathway at different disease points, which would be physiologically consistent with our animal observations that higher activation of the cGAS-IRF3 pathway leads to greater liver injury. However, it must be emphasized that our human analyses are correlative in nature.

cGAS-IRF3 activation and intercellular communication through hepatic gap junctions represent novel pathways for the induction and amplification of ALD. The role of gap junction–dependent communication in liver diseases is evolving, and our data highlight this pathway as an attractive therapeutic target for combating ALD.

Materials and Methods

ALD Patient Cohort Studies. Human liver samples were obtained from the Human Biorepository Core of the NIH-funded international InTeam Consortium. This cohort has been described previously, and data are available in the National Center for Biotechnology Information Database of Genotypes and Phenotypes (dbGAP) (20). All patients included gave written informed consent, and the research protocols were approved by the local Ethics Committees and by the central Institutional Review Board of the University of North Carolina at Chapel Hill. A total of 51 patients (all nonobese with high alcohol intake) were included and separated by disease phenotype: 1) early alcoholic steatohepatitis (ASH) (n = 12), mildly elevated serum aminotransferase levels and histologic evidence of steatohepatitis; 2) nonsevere ASH (n = 11), patients with histologically confirmed acute alcoholic hepatitis with a model for end-stage liver disease (MELD) <22; and 3) severe ASH (n = 18), patients with histologically confirmed acute alcoholic hepatitis with a MELD ≥22. All biopsies were performed prior to initiation of treatment. These groups were compared to nondiseased human livers (n = 10), either as an aggregate or individually by subtype. Patients with malignancies were excluded from the study. RNA extraction, sequencing, and bioinformatic analysis have been described previously (20). Analysis of differential expression was performed with the Limma R package (28). Pathway enrichment was performed by gene set enrichment analysis (GSEA) (29).

In Vivo Induction of Alcoholic Steatohepatitis. Female C57/BL6 (WT) mice aged 12 wk were obtained from Jackson Laboratory. Mice genetically deficient for Cx32 (Cx32KO) were obtained from K. Willecke (University of Bonn) and D. Paul (Harvard University). IRF3 KO mice were generated by Tadatsugu Taniguchi and obtained from E. Rosen (Harvard University). Hepatocyte-specific cGAS KO mice were generated with the Cre-Lox system. Mice expressing a floxed *cGas* exon 2 (cGAS F/F) were backcrossed to C57BL/6J mice (30). These mice were obtained from C. Rice (Rockefeller University). The mice were then crossed with albumin-Cre mice to create mice with cGAS deficiency only in hepatocytes (cGAS LKO). STING KO mice were obtained from H. Reinecker (Harvard University). To induce alcoholic hepatitis, we followed the protocol outlined in the National Institute on Alcohol Abuse and Alcoholism (NIAAA) chronic and binge model (31). To induce chronic alcohol-related liver disease, we used the classic Lieber-DeCarli model for 6 wk (21). Alcohol and PF diets were obtained from BioServ. To determine whether Cx32 deficiency offers survival benefit against ethanol-induced liver injury, we placed Cx32KO and WT mice, which were treated with 2APB at a dose of 20 mg/kg administered daily by intraperitoneal injection, on a 6% ethanol-containing liquid diet (32).

Data Availability. All relevant data supporting the findings of this study are available in the paper and supplemental materials. The data that support the findings of this study are available from the corresponding author on reasonable request. See *SI Appendix, Methods* for remaining methods.

1. J. M. Schwartz, J. F. Reinus, Prevalence and natural history of alcoholic liver disease. *Clin. Liver Dis.* **16**, 659–666 (2012).
2. E. Nguyen-Khac *et al.*; AAH-NAC Study Group, Glucocorticoids plus N-acetylcysteine in severe alcoholic hepatitis. *N. Engl. J. Med.* **365**, 1781–1789 (2011).
3. B. Gao *et al.*, Innate immunity in alcoholic liver disease. *Am. J. Physiol. Gastrointest. Liver Physiol.* **300**, G516–G525 (2011).
4. L. E. Nagy, The role of innate immunity in alcoholic liver disease. *Alcohol Res.* **37**, 237–250 (2015).
5. G. Szabo, J. Petrasek, S. Bala, Innate immunity and alcoholic liver disease. *Dig. Dis.* **30** (suppl. 1), 55–60 (2012).
6. H. Cichoż-Lach, A. Michalak, Oxidative stress as a crucial factor in liver diseases. *World J. Gastroenterol.* **20**, 8082–8091 (2014).
7. P. Stärkel, S. Leclercq, P. de Timary, B. Schnabl, Intestinal dysbiosis and permeability: The yin and yang in alcohol dependence and alcoholic liver disease. *Clin. Sci. (Lond.)* **132**, 199–212 (2018).
8. A. Ablasser *et al.*, cGAS produces a 2′-5′-linked cyclic dinucleotide second messenger that activates STING. *Nature* **498**, 380–384 (2013).
9. J. Bai, F. Liu, The cGAS-cGAMP-STING pathway: A molecular link between immunity and metabolism. *Diabetes* **68**, 1099–1108 (2019).
10. Y. Mao *et al.*, STING-IRF3 triggers endothelial inflammation in response to free fatty acid-induced mitochondrial damage in diet-induced obesity. *Arterioscler. Thromb. Vasc. Biol.* **37**, 920–929 (2017).
11. X. D. Li *et al.*, Pivotal roles of cGAS-cGAMP signaling in antiviral defense and immune adjuvant effects. *Science* **341**, 1390–1394 (2013).
12. S. R. Woo *et al.*, STING-dependent cytosolic DNA sensing mediates innate immune recognition of immunogenic tumors. *Immunity* **41**, 830–842 (2014).
13. J. Petrasek *et al.*, STING-IRF3 pathway links endoplasmic reticulum stress with hepatocyte apoptosis in early alcoholic liver disease. *Proc. Natl. Acad. Sci. U.S.A.* **110**, 16544–16549 (2013).
14. D. Segretain, M. M. Falk, Regulation of connexin biosynthesis, assembly, gap junction formation, and removal. *Biochim. Biophys. Acta* **1662**, 3–21 (2004).
15. S. J. Patel, K. R. King, M. Casali, M. L. Yarmush, DNA-triggered innate immune responses are propagated by gap junction communication. *Proc. Natl. Acad. Sci. U.S.A.* **106**, 12867–12872 (2009).
16. A. Ablasser *et al.*, Cell intrinsic immunity spreads to bystander cells via the intercellular transfer of cGAMP. *Nature* **503**, 530–534 (2013).
17. S. J. Patel *et al.*, Gap junction inhibition prevents drug-induced liver toxicity and fulminant hepatic failure. *Nat. Biotechnol.* **30**, 179–183 (2012).
18. J. Luther *et al.*, Hepatic connexin 32 associates with nonalcoholic fatty liver disease severity. *Hepatol. Commun.* **2**, 786–797 (2018).
19. R. Wang, F. Huang, Z. Chen, S. Li, Downregulation of connexin 32 attenuates hypoxia/reoxygenation injury in liver cells. *J. Biochem. Mol. Toxicol.* **29**, 189–197 (2015).
20. J. Argemi *et al.*, Defective HNF4alpha-dependent gene expression as a driver of hepatocellular failure in alcoholic hepatitis. *Nat. Commun.* **10**, 3126 (2019).
21. R. J. Wilkin, P. F. Lalor, R. Parker, P. N. Newsome, Murine models of acute alcoholic hepatitis and their relevance to human disease. *Am. J. Pathol.* **186**, 748–760 (2016).
22. A. P. West *et al.*, Mitochondrial DNA stress primes the antiviral innate immune response. *Nature* **520**, 553–557 (2015).
23. H. Kato *et al.*, Connexin 32 dysfunction promotes ethanol-related hepatocarcinogenesis via activation of Dusp1-Erk axis. *Oncotarget* **7**, 2009–2021 (2016).
24. M. R. Thursz *et al.*; STOPAH Trial, Prednisolone or pentoxifylline for alcoholic hepatitis. *N. Engl. J. Med.* **372**, 1619–1628 (2015).
25. N. Ohshima *et al.*, New members of the mammalian glycerophosphodiester phosphodiesterase family: GDE4 and GDE7 produce lysophosphatidic acid by lysophospholipase D activity. *J. Biol. Chem.* **290**, 4260–4271 (2015).
26. Z. Li *et al.*, Lysophosphatidylcholine acyltransferase 3 knockdown-mediated liver lysophosphatidylcholine accumulation promotes very low density lipoprotein production by enhancing microsomal triglyceride transfer protein expression. *J. Biol. Chem.* **287**, 20122–20131 (2012).
27. K. Takeuchi, K. Reue, Biochemistry, physiology, and genetics of GPAT, AGPAT, and lipin enzymes in triglyceride synthesis. *Am. J. Physiol. Endocrinol. Metab.* **296**, E1195–E1209 (2009).
28. M. E. Ritchie *et al.*, Limma powers differential expression analyses for RNA-sequencing and microarray studies. *Nucleic Acids Res.* **43**, e47 (2015).
29. A. Subramanian *et al.*, Gene set enrichment analysis: A knowledge-based approach for interpreting genome-wide expression profiles. *Proc. Natl. Acad. Sci. U.S.A.* **102**, 15545–15550 (2005).
30. J. W. Schoggins *et al.*, Pan-viral specificity of IFN-induced genes reveals new roles for cGAS in innate immunity. *Nature* **505**, 691–695 (2014).
31. A. Bertola, S. Mathews, S. H. Ki, H. Wang, B. Gao, Mouse model of chronic and binge ethanol feeding (NIAAA model). *Nat. Protoc.* **8**, 627–637 (2013).
32. J. Yanai, B. E. Ginsburg, Increased sensitivity to chronic ethanol in isolated mice. *Psychopharmacology (Berl.)* **46**, 185–189 (1976).